Pis'ma v ZhETF, vol. 101, iss. 7, pp. 512 – 517 © 2015 April 10

Anomalous Hall effect in MnSi: intrinsic to extrinsic crossover

V. V. Glushkov[+*1)], *I. I. Lobanova*[+*], *V. Yu. Ivanov*[+], *S. V. Demishev*[+*]

[+]*Prokhorov General Physics Institute of the RAS, 119991 Moscow, Russia*

[*]*Moscow Institute of Physics and Technology, 141700 Dolgoprudny, Russia*

Submitted 31 December 2014

Resubmitted 17 February 2015

Temperature dependences of low field Hall resistivity $\rho_{\rm H}$ are used to separate anomalous ($\rho^a_{\rm H}$) and normal ($R_{\rm H}B$) contributions to Hall effect in chiral magnet MnSi ($T_c \approx 29.1\,$K). It is found that the transition between paramagnetic ($T > T_c$) and magnetically ordered ($T < T_c$) phases is accompanied by the change in anomalous Hall resistivity from low temperature behavior governed by Berry phase effects ($\rho^a_{\rm H} = \mu_0 S_2 \rho^2 M$, $T < T_c$) to high temperature regime dominated by skew scattering ($\rho^a_{\rm H} = \mu_0 S_1 \rho M$, $T > T_c$). The crossover between the intrinsic ($\sim \rho^2$) and extrinsic ($\sim \rho$) contributions to anomalous Hall effect develops together with the noticeable increase of the charge carriers' concentration estimated from the normal Hall coefficient (from $n/n_{\rm Mn}(T > T_c) \approx 0.94$ to $n/n_{\rm Mn}(T < T_c) \approx 1.5$, $n_{\rm Mn} \approx 4.2 \cdot 10^{22}\,{\rm cm}^{-3}$). The observed features may correspond to the dramatic change in Fermi surface topology induced by the onset of long range magnetic order in MnSi.

DOI: 10.7868/S0370274X15070085

The unique combination of nontrivial physical properties makes the non-centrosymmetric B20 compound MnSi to be one of the most intriguing objects of contemporary condensed matter physics [1–3]. The intricate concurrence between ferromagnetic exchange, Dzyaloshinskii–Moriya (DM) interaction and spin-orbit coupling induces helimagnetic order appearing below $T_c \approx 29\,$K [4, 5]. Moderate pressure destroys this ground state ($T_c \approx 0\,$K at $p_c \approx 1.5\,$GPa) resulting in the transition into exotic magnetic phase with partial spin order and non-Fermi liquid behavior of resistivity [1, 6, 7]. The chiral DM interaction also favors to the formation of exotic topological spin texture – skyrmion lattice, which appears at ambient pressure in the A-phase near T_c [8]. The difference in Berry phases acquired by the spin-up and spin-down electrons under motion in the skyrmion lattice results in a topological contribution to Hall effect $\rho^t_{\rm H}$ [9], which was recently detected in MnSi and $Mn_{1-x}Fe_xSi$ [10–15]. This addition to Hall resistivity ranges from $\rho^t_{\rm H} \approx -30\,{\rm n}\Omega\cdot{\rm cm}$ to $\rho^t_{\rm H} \approx +50\,{\rm n}\Omega\cdot{\rm cm}$ [3, 10–15] and is believed to depend on the local spin polarization of band states, normal Hall constant and emergent magnetic field per skyrmion [11].

However, the separation between normal and anomalous contributions to Hall effect in MnSi is still controversial. The large amplitude of the anomalous Hall resistivity impedes the accurate determination of normal Hall constant $R_{\rm H}$ at low temperatures, which was reported to vary in the single crystals from $-7 \cdot 10^{-5}\,{\rm cm}^3/{\rm C}$ [12] to $-1.7 \cdot 10^{-4}\,{\rm cm}^3/{\rm C}$ [13] at 4.2 K. The uncertainty in the values of these different contributions to Hall effect in MnSi doesn't allow extracting any reliable information about the parameters of electron structure and scattering mechanisms of charge carriers, which could be significantly influenced by the correlation effects in the magnetic and paramagnetic phases of this compound [16, 17]. It is worth while noting that the standard procedure of the analysis of isothermal field dependencies of Hall resistivity and magnetization fails to extract anomalous component above the helimagnetic transition temperature [18]. As a result, there is no consensus about the origin of anomalous Hall effect in the paramagnetic state of MnSi, which is generally presented as some admixture of intrinsic (appearing due to Berry-phase effects in the momentum space $\rho^a_{\rm H} \sim \rho^2$) and extrinsic (induced by skew scattering of charge carriers $\rho^a_{\rm H} \sim \rho$) contributions [19, 20]. This ambiguous situation also puts into question the correctness of Hall effect analysis performed so far [10, 11, 13].

To shed more light on the origin of anomalous Hall effect in MnSi the temperature and field dependencies of Hall resistivity have been measured on the single crystal in magnetic fields below 5 T at temperatures 2–60 K. The quality of the crystal grown by Czochralski technique was checked by X-ray diffraction. As the magnetic properties of this compound depend strongly on the Mn/Si ratio [21], the special attention was paid

[1)]e-mail: glushkov@lt.gpi.ru

to the control of the sample's stoichiometry. EPMA data showed that the deviation from the stoichiometric composition doesn't exceed $y \approx 0.01$ assuming $Mn_{1+y}Si_{1-y}$ chemical formula. More detailed information about structural and magnetic properties can be found in the preceding studies of the single crystals, which are identical to those studied in the present work [7, 22–24]. The resistivity and Hall resistivity were measured simultaneously by using the standard six-probe scheme. The original technique with the step-by-step rotation of the sample in steady magnetic field was applied for the measurements of low-field Hall voltage within the 1–3 nV accuracy [25]. The axis of rotation was parallel to dc current (30–100 mA) applied along the $\langle 110 \rangle$ direction (see inset in Fig. 1). The size of the

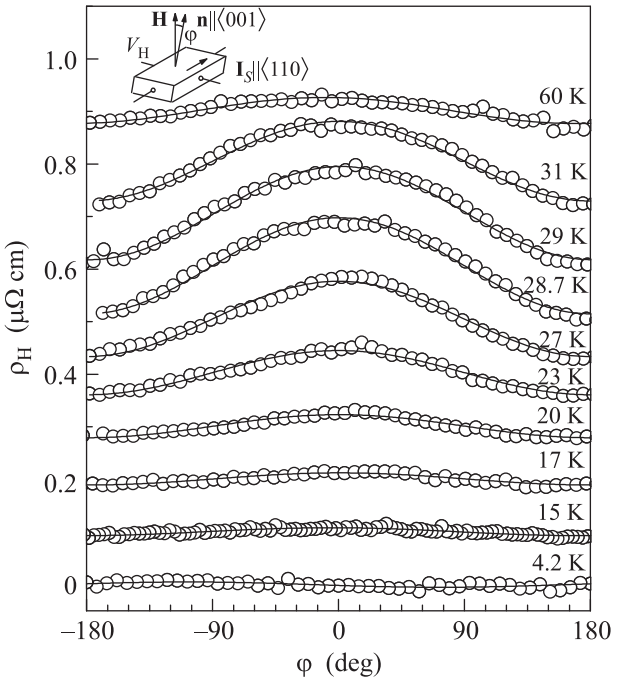

Fig. 1. Angular dependences of Hall resistivity $\rho_H(\varphi, T_0, H_0)$ measured for MnSi in applied magnetic field $\mu_0 H = 0.31$ T at temperatures 4.2–60 K. Solid lines are the fits by $\rho_H(\varphi) = \rho_H(T, B_0)\cos\varphi$. Inset presents the measuring sceme ($\mathbf{I}_S$ – dc current, V_H – Hall voltage, $\mathbf{n}$ – normal to the (001) plane and φ is the angle between $\mathbf{n}$ and applied magnetic field)

crystal ($5.2 \times 0.68 \times 0.54\,\text{mm}^3$) was chosen to minimize the anisotropy due to demagnetizing field. The demagnetization factor of the sample under investigation ($N \approx 0.52$) was evaluated within standard approach [26]. The magnetization data $M(H, T)$ earlier reported in [24] were collected with the help of MPMS-5 setup.

Fig. 1 presents selected angular dependencies of Hall resistivity ρ_H measured in external magnetic field $\mu_0 H_0 = 0.31$ T. The amplitude of Hall effect increases drastically when approaching T_c from low temperatures. The form of the signal is well described by the single harmonic of $\rho_H(\varphi) = \rho_H(T, H_0)\cos\varphi$, where φ is the angle between $\langle 100 \rangle$ and applied magnetic field (Fig. 1). In moderate fields ($\mu_0 H_0 > 2$ T) a second harmonic $\rho_{H2}(\varphi) = \rho_{H2}(T, H_0)\cos(2\varphi)$ appears distorting the form of Hall resistivity data. This feature, which is similar to that one earlier reported for the related compound FeSi [27], may correspond to the mechanism suggested in [28] and will be discussed in details elsewhere.

The extracted values of $\rho_H(T, H_0)$ were refined to allow for the demagnetization effects assuming the linear $\rho_H(H_0)$ and $M(H_0)$ dependencies in the range of magnetic fields $\mu_0 H_0 < 0.5$ T. The corrected temperature dependencies of Hall resistivity in a fixed magnetic field $\rho_H(T, B_0) = \rho_H(T, H_0)/[1 + (1 - N)M(H_0)/H_0)]$ are summarized in Fig. 2. Our presentation of the low-field data allows to resolve a pronounced peak of $\rho_H(T, B_0)$ occurring around T_c. This feature is much sharper that the anomaly of ρ_H^a reported for other correlated magnets [29]. The amplitude of the ρ_H maximum is found to rise from $+50\,\text{n}\Omega\cdot\text{cm}$ for $B_0 = 0.155$ T to $+95\,\text{n}\Omega\cdot\text{cm}$ for $B_0 = 0.31$ T (Fig. 2a–c). In higher magnetic fields the position of the maximum shifts to the paramagnetic phase and exceeds T_c by more than 10 K (see data for 4.04 T in Fig. 2). Note also that Hall effect in the magnetically ordered phase of MnSi changes sign from negative to positive when temperature increases from 2 K to T_c (Fig. 2). It is worth noting that the temperature evolution and the absolute values of Hall resistivity in MnSi agree well with the data reported earlier in [10, 11].

The strong temperature dependence of low-field Hall resistivity $\rho_H(T, B_0)$ in MnSi allows us to apply the following procedure for separating the normal and anomalous components $\rho_H = R_H B + \rho_H^a$. The functional form of the anomalous term $\rho_H^a = \mu_0 M S_n \rho^n$ depends on the dominant mechanism of interaction between itinerant electrons and localized magnetic moments [29]. In the case of MnSi the exponent $n = 2$ corresponds to the intrinsic contribution related to the k-space Berry phase effects [15]. Note that the same exponent $n = 2$ may result from extrinsic effects due to side-jump scattering [29]. This problem was carefully analysed in the studies of pure and Fe doped MnSi single crystals [15] and epitaxial MnSi thin films [20]. The sample-dependent contribution from side-jump scattering was shown to be negligibly small [20] that agrees rather well with the numerical estimations [15]. The case of $n = 1$ is associated with asymmetric skew scattering of spin-up and spin-down charge carriers on the magnetic cen-

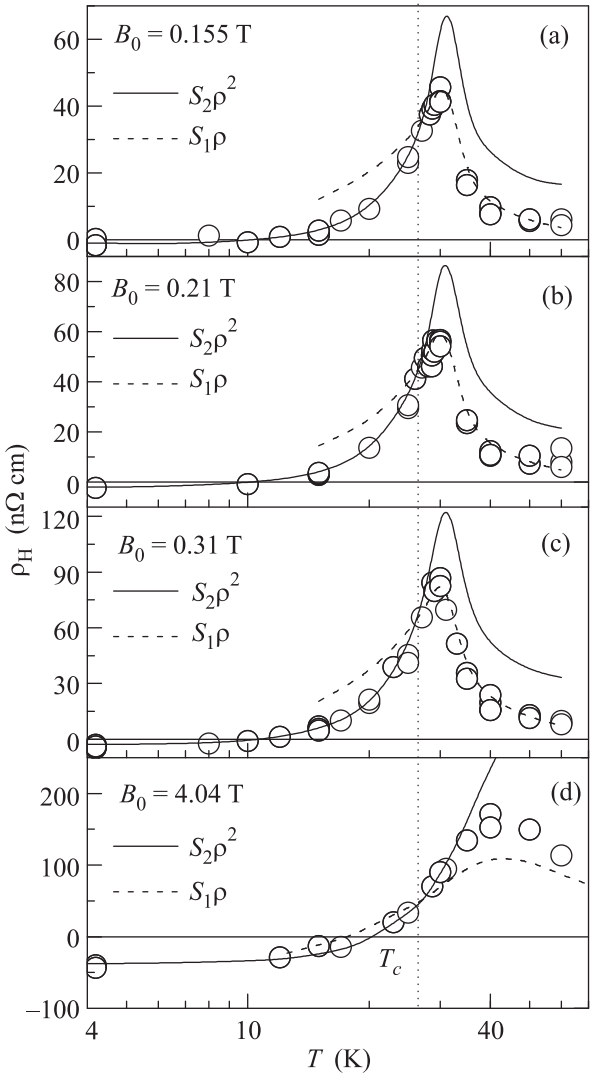

Fig. 2. Hall resistivity $\rho_H(T, B_0)$ in MnSi calculated from the $\rho_H(\varphi)$ data in magnetic fields $B_0 = 0.155\,\mathrm{T}$ (a), $0.21\,\mathrm{T}$ (b), $0.31\,\mathrm{T}$ (c) and $4.04\,\mathrm{T}$ (d). Solid and dashed lines correspond to the intrinsic ($T < T_c$) and extrinsic ($T > T_c$) regimes of anomalous Hall effect with the respective parameters $S_2 = 9.6 \cdot 10^2\,\Omega^{-1} \cdot \mathrm{cm}^{-1} \cdot \mathrm{T}^{-1}$, $R_H = -1.0 \cdot 10^{-4}\,\mathrm{cm}^3 \cdot \mathrm{C}^{-1}$ and $S_1 = 3.0 \cdot 10^{-2}\,\mathrm{T}^{-1}$, $R_H = -1.57 \cdot 10^{-4}\,\mathrm{cm}^3 \cdot \mathrm{C}^{-1}$ (see text). The experimental errors are within the symbol size

ters due to spin-orbit coupling [29]. To resolve between these regimes, we represented our data in $\rho_H/B = f(\mu_0 M\rho^2/B)$ (Fig. 3a) and $\rho_H/B = f(\mu_0 M\rho/B)$ plots (Fig. 3b). Fig. 3 demonstrates evidently that the data for magnetically ordered ($T < T_c$) and paramagnetic ($T > T_c$) phases should be described within the different approximations. In the range $T < T_c$ the best linearization of the ρ_H/B curves may be obtained in coordinates $\rho_H/B = R_H + \mu_0 M S_2 \rho^2/B$ with the

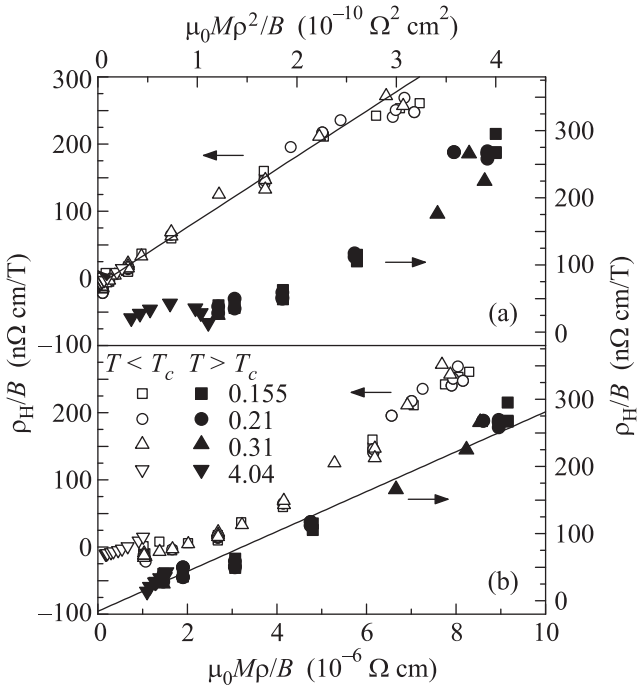

Fig. 3. Scaling plots of Hall resistivity $\rho_H/B = f(\rho^2\mu_0 M/B)$ (a) and $\rho_H/B = f(\rho\mu_0 M/B)$ (b). Open and solid symbols represent the data for $T < T_c$ and $T > T_c$, respectively. Solid lines are the linear fits of the experimental data (see text)

values of the parameters $R_H \approx -1.0 \cdot 10^{-4}\,\mathrm{cm}^3 \cdot \mathrm{C}^{-1}$ and $S_2 \approx 9.6 \cdot 10^2\,\Omega^{-1} \cdot \mathrm{cm}^{-1} \cdot \mathrm{T}^{-1}$. The analysis favors the intrinsic regime of the anomalous Hall effect in the spiral-based magnetically ordered phases of MnSi [10]. Additionally, our estimations are in good agreement with the values of R_H and S_2 reported earlier for $T < T_c$ [10, 11]. By the contrary, the best fit of the data in the paramagnetic state ($T > T_c$) corresponds to dependence $\rho_H/B = R_H + \mu_0 M S_2 \rho/B$ ($R_H \approx -1.57 \cdot 10^{-4}\,\mathrm{cm}^3 \cdot \mathrm{C}^{-1}$, $S_1 \approx 3.0 \cdot 10^{-2}\,\mathrm{T}^{-1}$, Fig. 3b) and therefore the anomalous Hall effect is defined by extrinsic factor contributed from skew scattering of charge carriers.

The crossover between the intrinsic and extrinsic regimes of anomalous Hall effect is clearly seen in Fig. 2, where solid and dashed lines show the fits $\rho_H = R_H B + \mu_0 M S_n \rho^n$ corresponding to the contributions from Berry phase effects $n = 2$ and skew scattering $n = 1$, respectively. Note that the maxima on the fits appear due to opposite trends in resistivity and magnetization with increasing of temperature. The experimental points are obviously described by the different fits below and above T_c (Fig. 2a–c). In our opinion, this finding proves the change in the scattering regimes of charge carriers occured under the onset of magnetic ordering. Note also that the crossover between the intrinsic and

extrinsic contributions to anomalous Hall effect happens in rather narrow temperature interval (28–31 K) near the Curie temperature.

The intrinsic to extrinsic crossover in anomalous Hall effect observed in MnSi is unusual for magnetic metals [29]. Generally, skew scattering prevails in good-metal limit ($\rho < 1\,\mu\Omega\cdot$cm), where anomalous Hall conductivity is proportional to transport relaxation time: $\sigma_{\rm H}^a \propto \tau \sim \sigma$ ($\rho_{\rm H}^a \sim \rho$) [29]. Increased impurity scattering diminishes τ so the intrinsic contribution from the Berry curvature ($\sigma_{\rm H}^a \sim {\rm const}(\tau)$, $\rho_{\rm H}^a \sim \rho^2$) is expected to become dominant at moderate resistivity ($1\,\mu\Omega\cdot{\rm cm} < \rho < 100\,\mu\Omega\cdot{\rm cm}$) [29]. This is not the case of MnSi where the $\rho_{\rm H}^a \sim \rho$ behavior is detected for rather high values of resistivity ($\sim 50\,\mu\Omega\cdot$cm [24]) and the Berry phase effects reveal only below T_c with a drastic decrease of resistivity (increase of relaxation time) [10, 13].

However, the widely used resistivity criterion for applicability of skew scattering model [29] cannot be considered as an absolute one. First of all, charge transport in the paramagnetic phase of MnSi ($T > T_c$) is controlled by scattering on magnetic fluctuations in the regime of strong exchange interaction between itinerant electrons and Mn localized magnetic moments [24]. Thus, the unique scattering mechanism determines the relaxation rate of charge carriers. Additionally, spin fluctuations may change their effective mass. Direct estimation of $m_{\rm eff}$ within single band approach using the obtained values of Hall mobility $|\mu_{\rm H}(30{-}60\,{\rm K})| = 2.3{-}3.8\,{\rm cm}^2/({\rm V}\cdot{\rm s})$ and scattering rate for the electronic continua in Raman spectra $\Gamma(\omega = 0) = 200 \pm 40\,{\rm cm}^{-1}$ [30] gives the relaxation rates $\tau = 0.12{-}0.17$ ps and the effective masses $m_{\rm eff} = 90 \pm 40 m_0$ (m_0 – free electron mass). This estimation of $m_{\rm eff}$ agrees reasonably with the values of $m_{\rm eff} \approx 18 m_0$ and $4{-}17 m_0$ known from de Haas-van Alphen (dHvA) oscillations [16] and optical conductivity [31], respectively. This discrepancy between dHvA and optical data and present estimate may be due to the fact that our case corresponds to low magnetic field/zero frequency limit. Consequently, the relatively high values of resistivity in the paramagnetic phase may have contributions from both effective mass and scattering time so that the straightforward use of the resistivity criterion [29] may be ambiguous.

The analysis of the experimental data obtained in this work shows that the $\rho_{\rm H}^a \propto M\rho$ regime develops in the paramagnetic phase with strong spin fluctuations. Previous studies [24] have revealed that spin fluctuations in the paramagnetic phase play a specific role making individual scattering processes on the magnetic centers to be independent. This gives the way for the implementation of the classical Yosida mechanism of negative magnetoresistance [24]. Consequently, the independent scattering $\rho_{\rm H}^a \propto M\rho$ seems to correspond to less correlated situation whereas the regime $\rho_{\rm H}^a \propto M\rho^2$ is observed in the case characterized by strong correlations in both spin orientation and scattering processes. It is worth noting that clean (good-metal) limit, where skew scattering may be observed, is associated with low impurities concentrations, where correlations between the individual scattering acts could be neglected [29]. Therefore, the observed intrinsic to extrinsic crossover in anomalous Hall effect in MnSi may be attributed to the change of the spin fluctuations rate in the vicinity of T_c.

In order to check the hypothesis we have examined the field dependences of Hall resistivity (Fig. 4). Within

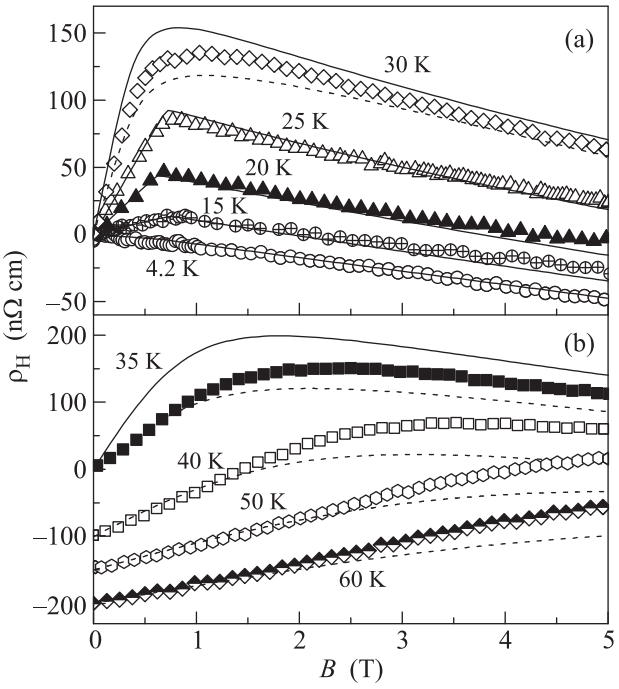

Fig. 4. Hall resistivity $\rho_{\rm H}(B, T_0)$ in MnSi in magnetic fields below 5 T at temperatures 4.2–30 K (a) and 35–60 K (b). Solid and dashed lines are the fits by $\rho_{\rm H} = R_{\rm H}B + S_2\rho^2\mu_0 M$ and $\rho_{\rm H} = R_{\rm H}B + S_1\rho\mu_0 M$, respectively. For clarity, the data for 40, 50 and 60 K in panel (b) are shifted down by 100, 150, and 200 $\mu\Omega\cdot$cm, respectively

the suggested approach, the increase of magnetic field leads to suppression of spin fluctuations and therefore the skew scattering asymptotic should be violated in strong magnetic field. Below T_c the simulations of the $\rho_{\rm H}(B)$ curves with the help of the low-field parameters fit the experimental data very well (Fig. 4a). In the crossover region $T = 30\,{\rm K} \sim T_c$ both asymptotics $\rho_{\rm H}^a \propto M\rho$ and $\rho_{\rm H}^a \propto M\rho^2$ demonstrate noticeable dis-

crepancies with the experimental curve (Fig. 4a). It is most interesting that in the paramagnetic phase the intrinsic model fails completely in the approximation of the $\rho(B)$ data (solid line in Fig. 4b). At the same time low-field skew scattering approximation for $T > T_c$ meets the experimental situation only for $B < 1.5\,\mathrm{T}$ (dashed lines in Fig. 4b). This discrepancy can be hardly attributed to the hypothetical presence of several kinds of charge carriers. Indeed, the magnetoresistance scaling $\Delta\rho/\rho = a_0 M^2$ ($a_0 = \mathrm{const}(T, B)$) to be specific for the paramagnetic phase of MnSi for $B < 8\,\mathrm{T}$ and $T_c < T < 80\,\mathrm{K}$ [24] suggests the dominating contribution to the charge transport from the single group of electrons. Consequently, the deviations of the experimental $\rho(B)$ curves from the skew scattering model above $B \approx 1{-}2\,\mathrm{T}$ may be reasonably associated with the expected altering of the extrinsic scattering due to suppression of spin fluctuations.

In this situation the crossover between extrinsic ($T > T_c$) and intrinsic ($T < T_c$) regimes of anomalous Hall effect in MnSi can be considered in terms of the electronic structure transformation under the onset of long-range magnetic order, which damps also the effects of spin fluctuations. This suggestion is proved by the rapid decrease of normal Hall effect that takes place near the Curie temperature. Our data show that below this point the absolute value of normal Hall constant decreases by more than 30 % from $R_\mathrm{H} \approx -1.57 \times \times 10^{-4}\,\mathrm{cm}^3/\mathrm{C}$ down to $R_\mathrm{H} \approx -1.0 \cdot 10^{-4}\,\mathrm{cm}^3/\mathrm{C}$. Note that $R_\mathrm{H}(T > T_c)$ estimated from our data agrees well with normal Hall constant $R_\mathrm{H} \approx -1.67 \cdot 10^{-4}\,\mathrm{cm}^3/\mathrm{C}$ earlier reported for room temperatures [11]. So magnetic ordering in MnSi seems to increase the effective concentration of charge carriers, which rises from $n/n_\mathrm{Mn} \approx 0.94$ at $T > T_c$ to $n/n_\mathrm{Mn} \approx 1.5$ at $T < T_c$ ($n_\mathrm{Mn} \approx 4.2 \cdot 10^{22}\,\mathrm{cm}^{-3}$). In our opinion, the possible realization of the electronic transition in MnSi may be independently checked by high precision electron photoemission studies.

Summarizing up, anomalous (ρ^a_H) and normal ($R_\mathrm{H}B$) contributions to Hall effect in chiral magnet MnSi have been separated from the analysis of the temperature dependences of Hall resistivity $\rho_\mathrm{H}(T)$ in low magnetic fields. Increasing temperature is shown to result in the transition from the behavior of the anomalous Hall resistivity governed by the Berry phase effects ($\rho^a_\mathrm{H} = \mu_0 S_2 \rho^2 M$, $T < T_c$) to the regime dominated by skew scattering ($\rho^a_\mathrm{H} = \mu_0 S_1 \rho M$, $T > T_c$). The noticeable increase of the charge carriers' concentration accompanied the crossover between the intrinsic ($\sim \rho^2$) and extrinsic ($\sim \rho$) regimes of anomalous Hall effect points to the dramatic change in charge carriers scattering and Fermi surface topology induced by the onset of helimagnetic order in MnSi.

The authors are grateful to S.M. Stishov for valuable discussions at the early stage of the work and to N.E. Sluchanko for critical comments and stimulating discussions. This research was supported by the RAS Program "Strongly correlated electrons" and RFBR project # 13-02-00160-a.

1. C. Pfleiderer, S. R. Julian, and G. G. Lonzarich, Nature **414**, 427 (2001).
2. S. M. Stishov and A. E. Petrova, Physics-Uspekhi **54**, 1117 (2011).
3. R. Ritz, M. Halder, M. Wagner, C. Franz, A. Bauer, and C. Pfleiderer, Nature **497**, 231 (2013).
4. Y. Ishikawa, K. Tajima, D. Bloch, and M. Roth, Sol. State Comm. **19**, 525 (1976).
5. O. Nakanishi, A. Yanase, A. Hasegawa, and M. Kataoka, Sol. State Comm. **35**, 995 (1980).
6. C. Pfleiderer, D. Reznik, L. Pintschovius, H. v. Löhneysen, M. Garst, and A. Rosch, Nature **427**, 227 (2004).
7. A. E. Petrova and S. M. Stishov, Phys. Rev. **B86**, 174407 (2012).
8. S. Mühlbauer, B. Binz, F. Jonietz, C. Pfleiderer, A. Rosch, A. Neubauer, R. Georgii, and P. Böni, Science **323**, 915 (2009).
9. D. Xiao, M. C. Chang, and Q. Niu, Rev. Mod. Phys. **82**, 1959 (2010).
10. M. Lee, Y. Onose, Y. Tokura, and N. P. Ong, Phys. Rev. B **75**, 172403 (2007).
11. A. Neubauer, C. Pfleiderer, B. Binz, A. Rosch, R. Ritz, P. G. Niklowitz, and P. Böni, Phys. Rev. Lett. **102**, 186602 (2009).
12. M. Lee, W. Kang, Y. Onose, Y. Tokura, and N. P. Ong, Phys. Rev. B **102**, 186601 (2009).
13. R. Ritz, M. Halder, C. Franz, A. Bauer, M. Wagner, R. Bamler, A. Rosch, and C. Pfleiderer, Phys. Rev. B **87**, 134424 (2013).
14. T. Yokouchi, N. Kanazawa, A. Tsukazaki, Y. Kozuka, M. Kawasaki, M. Ichikawa, F. Kagawa, and Y. Tokura, Phys. Rev. B **89**, 064416 (2014).
15. C. Franz, F. Freimuth, A. Bauer, R. Ritz, C. Schnarr, C. Duvinage, T. Adams, S. Blügel, A. Rosch, Y. Mokrousov, and C. Pfleiderer, Phys. Rev. Lett. **112**, 186601 (2014).
16. G. G. Lonzarich, J. Magn. Magn. Mater. **76–77**, 1 (1988).
17. V. G. Storchak, J. H. Brewer, R. Ł. Lichti, Th. A. Lograsso, and D. Ł. Schlagel, Phys. Rev. B **83**, 140404 (2011).
18. A. Neubauer, C. Pfleiderer, R. Ritz, P. G. Niklowitz, and P. Böni, Physica B **404**, 3163 (2009).

19. B. J. Chapman, M. G. Grossnickle, T. Wolf, and M. Lee, Phys. Rev. B **88**, 214406 (2013).
20. Y. Li, N. Kanazawa, X. Z. Yu, A. Tsukazaki, M. Kawasaki, M. Ichikawa, X. F. Fin, F. Kagawa, and Y. Tokura, Phys. Rev. Lett. **110**, 117202 (2013).
21. V. V. Rylkov, S. N. Nikolaev, K. Yu. Chernoglazov, B. A. Aronzon, K. I. Maslakov, V. V. Tugushev, E. T. Kulatov, I. A. Likhachev, E. M. Pashaev, A. S. Semisalov, N. S. Perov, A. B. Granovskii, E. A. Ganshina, O. A. Novodvorskii, O. D. Khramova, E. V. Khaidukov, and V. Ya. Panchenko, JETP Lett. **96**, 255 (2012).
22. A. E. Petrova, V. N. Krasnorussky, A. A. Shikov, W. M. Yuhasz, T. A. Lograsso, J. C. Lashley, and S. M. Stishov, Phys. Rev. B **82**, 155124 (2010).
23. S. V. Demishev, A. V. Semeno, A. V. Bogach, V. V. Glushkov, N. E. Sluchanko, N. A. Samarin, and A. L. Chernobrovkin, JETP Lett. **93**, 213 (2011).
24. S. V. Demishev, V. V. Glushkov, I. I. Lobanova, M. A. Anisimov, V. Yu. Ivanov, T. V. Ishchenko, M. S. Karasev, N. A. Samarin, N. E. Sluchanko, V. M. Zimin, and A.V. Semeno, Phys. Rev. B **85**, 045131 (2012).
25. N. E. Sluchanko, A. V. Bogach, V. V. Glushkov, S. V. Demishev, M. I. Ignatov, N. A. Samarin, G. S. Burkhanov, and O. D. Chistyakov, JETP **98**, 793 (2002).
26. A. Aharoni, J. Appl. Phys. **83**, 3432 (1998).
27. V. V. Glushkov, I. B. Voskoboinikov, S. V. Demishev, I. V. Krivitskii, A. Menovsky, V. V. Moshchalkov, N. A. Samarin, and N. E. Sluchanko, JETP **99**, 394 (2004).
28. B. Binz and A. Vishwanath, J. Magn. Magn. Mater. **310**, 1062 (2007).
29. N. Nagaosa, J. Sinova, S. Onoda, A. H. MacDonald, and N. P. Ong, Rev. Mod. Phys. **82**, 1539 (2010).
30. H.-M. Eiter, P. Jaschke, R. Hackl, A. Bauer, M. Gangl, and C. Pfleiderer, Phys. Rev. **B90**, 024411 (2014).
31. F. Mena, D. van der Marel, A. Damascelli, M. Fäth, A. Menovsky, and J. Mydosh, Phys. Rev. B **67**, 241101 (2003).